

Separable Convolutional Eigen-Filters (SCEF): Building Efficient CNNs Using Redundancy Analysis

Samuel Scheidegger *

Chalmers University of Technology, Sweden

Yinan Yu *

Chalmers University of Technology, Sweden

Tomas McKelvey

Chalmers University of Technology, Sweden

Abstract

The high model complexity of deep learning algorithms enables remarkable learning capacity in many application domains. However, a large number of trainable parameters comes with a high cost. For example, during both the training and inference phases, the numerous trainable parameters consume a large amount of resources, such as CPU/GPU cores, memory and electric power. In addition, from a theoretical statistical learning perspective, the high complexity of the network can result in a high variance in its generalization performance. One way to reduce the complexity of a network without sacrificing its accuracy is to define and identify redundancies in order to remove them. In this work, we propose a method to observe and analyze redundancies in the weights of a 2D convolutional (Conv2D) network. Based on the proposed analysis, we construct a new layer called Separable Convolutional Eigen-Filters (SCEF) as an alternative parameterization to Conv2D layers. A SCEF layer can be easily implemented using depthwise separable convolution, which are known to be computationally effective. To verify our hypothesis, experiments are conducted on the CIFAR-10 and ImageNet datasets by replacing the Conv2D layers with SCEF and the results have shown an increased accuracy using about 2/3 of the original parameters and reduce the number of FLOPs to 2/3 of the original net. Implementation-wise, our method is highly modular, easy to use, fast to process and does not require any additional dependencies.

1. Introduction

Deep learning is a highly complex modelling technique that potentially results in low bias but high variance in its generalization accuracy. The large number of trainable parameters implies extremely high computational complexity,

which requires renting or purchasing expensive infrastructure for training. Moreover, the runtime of a trained network plays an important role for time critical applications, such as data analysis and decision making in medical domains and autonomous driving applications. With a large amount of parameters, it may violate the runtime constraint of the application. Therefore, model reduction steps could be beneficial in terms of computational efficiency and reduced overall cost for deep learning. One of the most classic model reduction methods is the subspace low rank approximation (Belhumeur et al. [2], Jolliffe [19], Golub and van Loan [8]). It is a family of very well studied and widely used techniques in the area of signal processing and machine learning. The main concept is to arrange the trainable variables into a vector space and find a subspace spanned by the most significant singular vectors of these variables. The idea of this paper is to combine the subspace technique and deep learning to achieve a desirable ratio between the size of the network and the generalization accuracy. Based on our observation that 2D convolutional (Conv2D) filters exhibit low rank behaviors in a trained network, we propose a new layer structure called Separable Convolutional Eigen-Filters (SCEF) using subspace approximation techniques in combination with depthwise separable convolutions as an alternative parameterization of the filters in Conv2D layers.

In this paper, we illustrate two use cases of SCEF layers and validate our hypotheses by showing experiments conducted on the standard datasets CIFAR-10 and ImageNet. To better understand the properties of SCEF, we conduct ablation studies on the smaller dataset CIFAR-10. The results show an increased accuracy while using about two thirds of the base network. We then apply the algorithms to a larger dataset ImageNet and observe similar results. In addition to reducing the network complexity, the SCEF layer and its algorithms have the following properties:

1. Modularity: SCEF is essentially a filter structure. A filter is the smallest element in a Convolutional Neural Network (CNN). By manipulating each filter, the layer

*These authors contributed equally to this work.

representation is not tied to a specific network topology, which allows a flexible and modular design.

2. Reproducibility: Our effort to increase the reproducibility lies in three aspects.

Implementation: The proposed algorithms are easily implemented by the depthwise separable convolution that was recently made available in most popular deep learning frameworks.

Dependencies: The SCEF layer and its algorithms require no additional dependencies (e.g. libraries, optimization algorithms) compared to Conv2D layers.

Deterministic rules for the hyperparameters: We use a rule-based approach for finding the hyperparameters to avoid the common problem of over-tuning in deep learning and to increase reproducibility. The rules for the hyperparameters are determined by cross-validation on a small dataset and directly applied to larger datasets without any adjustment or tuning.

3. Reasonability: With our observations and analyses of the low rank behaviors, we gain insights of the CNN network structure, which turns out to be effective factors in network design based on empirical verification.

Given these properties, our **contribution** is threefold.

- (1) While most previous subspace techniques mainly focus on compressing networks after training, our approach is primarily aiming at enabling the users to **build a network from scratch with trainable eigen-filters**. Given the modularity of the SCEF layers and the **deterministic rules for hyperparameters**, it is very easy to implement your own SCEF network and to reproduce our results.
- (2) We observe and analyze the Conv2D from a different perspective, which is motivated by the empirical evidence from our experiments. This opens up **new opportunities of understanding the design of convolutional networks and their redundancies**. Due to our observations of the low rank behaviors in the vector space constructed by vectorizing each individual filter, we construct the vector space differently from the existing work as follows: i). We vectorize the filters instead of using separable basis in the original vector space (Jaderberg et al. [18], Tai et al. [29], Ioannou et al. [17], Yu et al. [33]); ii) we do not concatenate these vectorized filters into a large vector space (Denton et al. [7], Wen et al. [30], Peng et al. [26]), which achieves a better modularity compared to the concatenated vectors.

(3) Depthwise separable convolution has became popular due to its computational efficiency (Chollet [4]). Our study shows a **design principle for depthwise separable convolutional layers**: one does not need more intermediate filters in depthwise separable convolutional layers than the filter size $K = h^2$ (e.g. $h = 3, K = 9$). It is better to increase the number of coefficients (i.e. the output channels) instead. The reason behind this is that we model the intermediate filters in depthwise separable convolutional layers as the K dimensional basis vectors of the corresponding Conv2D layer. Hence, a corollary is that we only need maximum K (independent) intermediate filters to represent any output.

Furthermore, we have gained interesting insights from these analyses, which are beneficial for further understanding and finding new design principles of CNNs.

2. SCEF Layers

2.1. Motivation

First, let us formally define what a “layer” is in this context.

Definition 1. *In the scope of this paper, a layer*

$$\mathcal{W} = \left\{ \mathbf{w}_j^{(i)} \in \mathbb{R}^{h \times h} : i = 1 \dots c_{in}, j = 1 \dots c_{out} \right\}$$

is a set of trainable units that are characterized by the following attributes: 1) number of input channels c_{in} ; 2) number of output channels c_{out} , and 3) parameterization (i.e. filter): $\mathbf{w}_j^{(i)} \in \mathbb{R}^{h \times h}$.

Note that there are multiple layers in a network, but we ignore the layer index in this definition for simplicity. However, when multiple layers appear in the same context, we use $\mathcal{W}_l, l \in \{1, \dots, L\}$ to denote the indexed layer throughout the paper. In addition, since the filter size h is not of our interest, we simply denote $K := h^2$ without loss of generality. In practice, the filter shape can be a rectangle. Moreover, for the sake of both consistency and convenience, we use i and j to denote the input channel index and the output channel index (i.e. the number of filters in a Conv2D layer), respectively.

Our motivation of this work originates from the low rank behaviors we have observed in the vectorized filter parameters, so let us start with this experimental procedure.

Procedure 1. *Analysis using Singular Value Decomposition (SVD)*

- *Apply vectorization $\bar{\mathbf{w}}_j^{(i)} = \text{vec}(\mathbf{w}_j^{(i)}) \in \mathbb{R}^K$ and compute the truncated SVD:*

$$\bar{\mathbf{U}}^{(i)} \mathbf{S}^{(i)} \mathbf{V}^{(i)T} = \begin{bmatrix} \bar{\mathbf{w}}_1^{(i)} & \dots & \bar{\mathbf{w}}_{c_{out}}^{(i)} \end{bmatrix}, \quad (1)$$

where matrices $\bar{\mathbf{U}}^{(i)}$ and $\mathbf{V}^{(i)}$ are the left and right singular matrix, respectively; and $\mathbf{S}^{(i)}$ is a diagonal matrix that contains the singular values in a descending order.

- Identify effective rank:

$$r_i = |\{ \mathbf{S}^{(i)}[k, k] : \mathbf{S}^{(i)}[k, k] \geq \gamma \mathbf{S}^{(i)}[1, 1], k = 1, \dots, \min(K, c_{out}), \gamma \in [0, 1] \}| \quad (2)$$

where $|\cdot|$ denotes the cardinality of a set and $\mathbf{M}[k, k]$ is the k^{th} diagonal element of matrix \mathbf{M} .

This procedure is demonstrated in Fig. 1. Empirical examples can be found in Fig. 2 for ResNet-32 trained on dataset CIFAR-10 and in Fig. 3 for ResNet-50 trained on dataset ImageNet, respectively. The figure shows the singular values computed using Eq. (1). Each row in a matrix represents the singular values for one input channel i . There are $K = h^2 = 9$ (3×3 is a commonly chosen filter size in ResNet) elements in each row due to the fact that $\min(K, c_{out}) = K$. The number of rows in each matrix equals to the number of input channels c_{in} . For convenience, we call each matrix in Fig. 2 $\mathbf{M} \in \mathbb{R}^{c_{in} \times 9}$ and denote each row of \mathbf{M} using $\mathbf{M}(i, :)$. For visualization purposes, the largest singular value of each matrix is normalized to one, i.e., $\mathbf{M} \leftarrow \frac{\mathbf{M}}{\|\mathbf{M}\|_\infty}$. The rows are sorted with respect to the largest singular value of each row in an ascending order, i.e., $\mathbf{M}(1, 1) \leq \mathbf{M}(2, 1) \leq \dots \leq \mathbf{M}(c_{in}, 1) = 1$. The gradient in $\mathbf{M}(i, :)$ shows the drop in the singular values. In Fig. 2 and Fig. 3, we observe many sharp drops in $\mathbf{M}(i, :)$, which indicate a low rank behavior in that input channel i .

Given these observations, we aim at finding approximations of these low rank filters, where the number of trainable parameters and FLOPs will be largely reduced.

2.2. Definition and properties

Generally speaking, subspace techniques bring better robustness to the learning system due to their reduced model complexity. Motivated by these observations and analyses, we define a SCEF layer as follows.

Definition 2 (SCEF layer). A SCEF (Separable Convolutional Eigen-Filters) layer is defined by

$$\Theta = \left\{ \mathbf{w}_j^{(i)}, \mathbf{w}_j^{(i)} \in \mathbb{R}^{h \times h}, i = 1 \dots c_{in}, j = 1 \dots c_{out} \right\}$$

with the following parameterization

$$\mathbf{w}_j^{(i)} = \sum_{k=1}^r a_{k,j}^{(i)} \mathbf{u}_k^{(i)}, \quad r \in [1, h^2] \quad (3)$$

where $a_{k,j}^{(i)} \in \mathbb{R}$ and $\mathbf{u}_k^{(i)} \in \mathbb{R}^{h \times h}$, which satisfy

$$\bar{\mathbf{u}}_l^{(i)T} \bar{\mathbf{u}}_m^{(i)} = \begin{cases} 1 & \text{if } l = m \\ 0 & \text{otherwise} \end{cases}$$

for $\bar{\mathbf{u}}_k^{(i)} = \text{vec}(\mathbf{u}_k^{(i)}) \in \mathbb{R}^{h^2}$. The parameters $\mathbf{u}_k^{(i)} \in \mathbb{R}^{h \times h}$ are called the **eigen-filters**.

Note that for the sake of clarity, we use Θ to denote the SCEF layer, instead of the generic notation \mathcal{W} in Def. 1.

In practice, SCEF can be implemented using the depth-wise separable convolution [4] that was recently made available in most deep learning frameworks. A SCEF layer has the following properties.

Property 1. Robustness

Lemma 1. Let $\Delta \mathbf{I}_i$ be an additive perturbation matrix and $\mathbf{w}_j^{(i)} \in \mathbb{R}^{h \times h}$ be a filter parameterized by Eq. (3), which is learned from some training process. Let

$$\bar{\mathbf{U}}^{(i)} = \left[\bar{\mathbf{u}}_0^{(i)}, \dots, \bar{\mathbf{u}}_r^{(i)} \right]. \quad (4)$$

If $\bar{\mathbf{U}}^{(i)T} \bar{\mathbf{U}}^{(i)} = \mathbf{I}$ and $\left\| \mathbf{a}_j^{(i)} \right\|_2 \leq \epsilon, \forall i, j$,

$$\left\| \sum_i \Delta \mathbf{I}_i * \mathbf{w}_j^{(i)} \right\|_\infty \leq \epsilon h r \sum_i \|\Delta \mathbf{I}_i\|_2. \quad (5)$$

Proof. See the supplementary material. \square

The robustness in this context is indicated by the propagation of the additive perturbation between input and output feature maps. Lemma 1 shows that when (1) $\bar{\mathbf{U}}^{(i)T} \bar{\mathbf{U}}^{(i)} = \mathbf{I}$, i.e. the vectorized filters are orthonormal, and (2) $\left\| \mathbf{a}_j^{(i)} \right\|_2 \leq \epsilon$, i.e. the coefficients are bounded by ϵ , the effect of the perturbation on the output is bounded by Eq. (5). The design parameter rank r of the eigen-filters controls a trade-off between the robustness and the representational power of a SCEF layer.

Property 2. Complexity (one layer)

- Number of trainable parameters (N)

– $N(\text{Conv2D})$: $c_{in} c_{out} h^2$

– $N(\text{SCEF})$:

– Eigen-filters: $N_u = c_{in} h^2 r$

– Coefficients: $N_a = c_{in} c_{out} r$

When $r = h^2$, randomly initialized eigen-filters can span the whole vector space and hence the eigen-filters do not need to be trainable, i.e. $N_u = 0$. Hence, Conv2D and SCEF are equivalent for $r = h^2$.

When $r < h^2$, $N(\text{SCEF}) < N(\text{Conv2D})$ if $r \leq \left\lfloor \frac{c_{out} h^2}{c_{out} + h^2} \right\rfloor$.

Example. Given $c_{in} = c_{out} = 128$ and $h = 3$, we have $N(\text{Conv2D}) = 147456$. If $r \leq 8$, then $N(\text{SCEF}) < N(\text{Conv2D})$. For $r = 8$, $N(\text{SCEF}) = 140288$ and for $r = 4$, $N(\text{SCEF}) = 70144$.

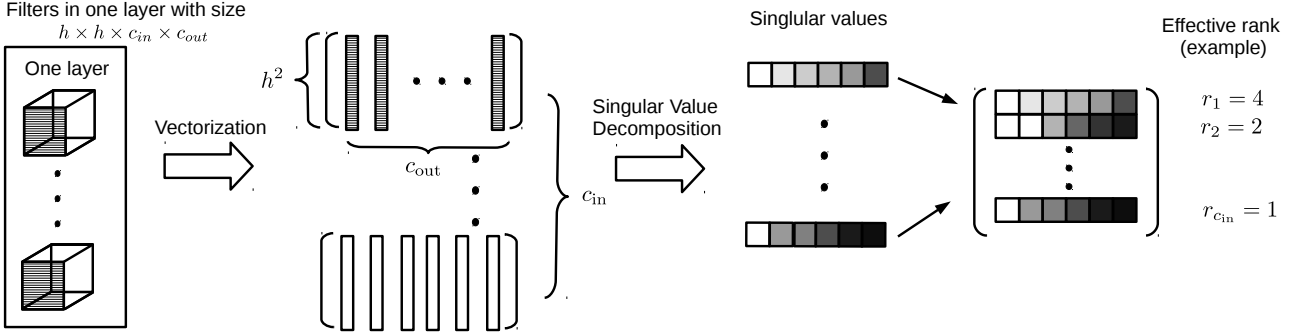


Figure 1: An illustration of how we observe the low rank behaviors in the layers.

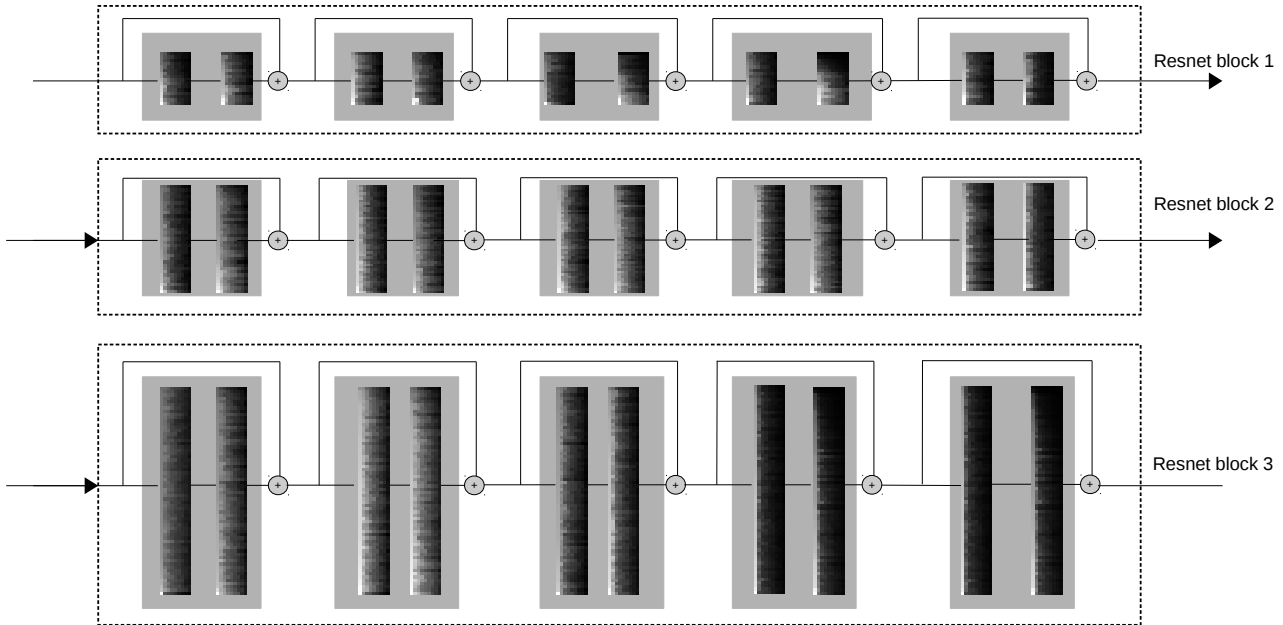


Figure 2: Singular values computed from ResNet-32 trained on CIFAR-10. The network is composed of three Resnet blocks. Within each block, the layers are grouped two-by-two with a residual connection. Each rectangle in this figure indicates one layer, where each row represents the singular values computed using Eq. (1). The procedure of these computations is demonstrated in Fig 1. We use a shaded background to highlight the drop in the non zero singular values, which indicates a low rank behavior.

- *FLOPs (F)*

We count the multiply-accumulate operations (macc) and we do not include bias in our calculations. Given the dimension of the input layer $H \times W \times c_{in}$, let $t = \lfloor \frac{H}{\text{stride}} \rfloor \times \lfloor \frac{W}{\text{stride}} \rfloor$,

- $F(\text{Conv2D})$: $th^2 c_{in} c_{out}$
- $F(\text{SCEF})$: $tc_{in}r (h^2 + c_{out})$

Example. Given $H = W = 100$, $c_{in} = 128$, $c_{out} = 128$ and $h = 3$ with $\text{stride} = 1$, we have $F(\text{Conv2D}) = 1.47 \text{ GFLOPs}$. For $r = 8$, $F(\text{SCEF}) = 1.40 \text{ GFLOPs}$.

For $r = 4$, $F(\text{SCEF}) = 0.70 \text{ GFLOPs}$.

2.3. Algorithms and Use Cases

In this paper, we explore two main use cases of SCEF layers: to build a network from scratch or to compress a trained network. The first use case is the one we recommend, where no pre-training is required. On the other hand, the compression use case is useful when a CNN is already trained and re-training is too costly, but one needs to reduce the runtime complexity.

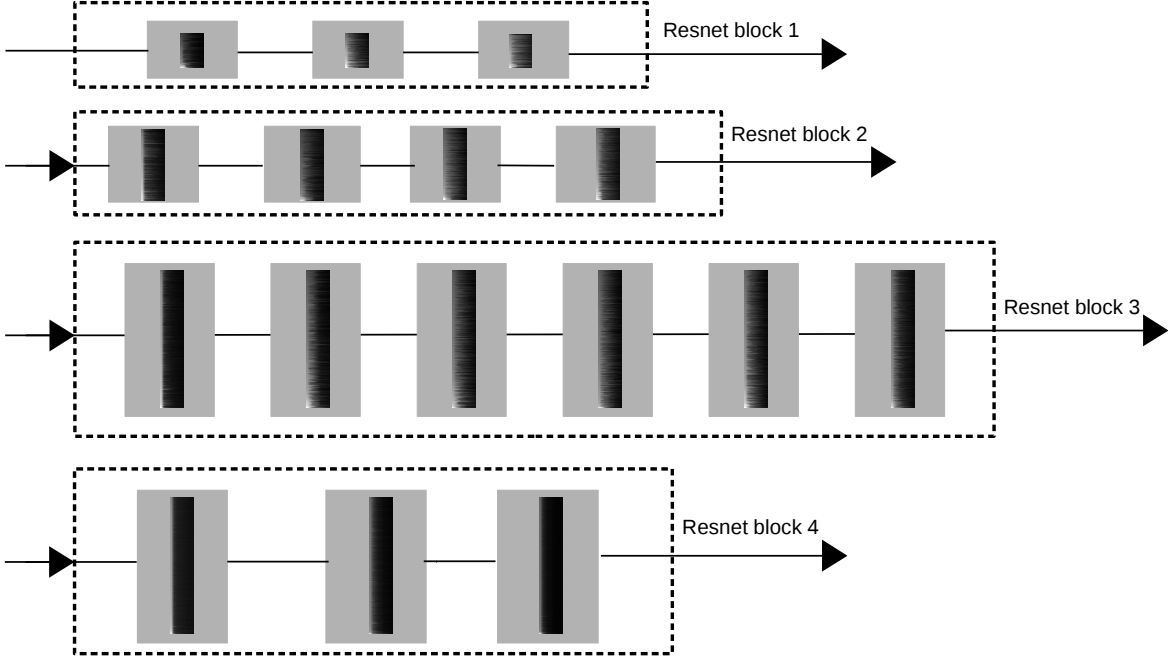


Figure 3: Singular values computed from ResNet-50 trained on ImageNet. Each row in the matrix represent the singular values computed using Eq. (1). The process of these computations is demonstrated in Fig 2. We use a shaded background to highlight the none zero singular values (with bright color) to visualize the drop of these singular values, which indicates low rank behaviors.

2.3.1 Use case 1 (recommended): building a network with trainable eigen-filters

Given any topology of a CNN, we replace the parameterization of Conv2D layers with SCEF and train the network from scratch. We show in the experiment section that the resulting network has a largely reduced number of trainable parameters and FLOPs compared to its Conv2D counterpart. Without loss of generality, we use a base network (e.g. ResNet) to indicate which topology we are using, while in practice, the topology can be arbitrarily chosen. For convenience, given a base network topology, we call the new network SCEF-basenet.

Training strategy Let f be a loss function for a given CNN architecture. We introduce a mapping:

$$g_{\Theta_l} : \mathbb{R}^{M^l \times N^l \times c_{\text{out}}^l} \longrightarrow \mathbb{R}^{M^{l+1} \times N^{l+1} \times c_{\text{out}}^{l+1}}$$

that represents the forward path between layer l and $l + 1$. We denote the regular CNN layer and SCEF layers using \mathcal{W}_l and Θ_l , respectively. Let $\mathcal{L} = \{1, \dots, L\}$ be the set of all the layer indices and $\mathcal{L}_g \subseteq \mathcal{L}$. For a given \mathcal{L}_g , the optimization problem we are trying to address is formulated

as follows:

$$\underset{\Theta_l, l \in \mathcal{L}_g, \mathcal{W}_q, q \in \mathcal{L} \setminus \mathcal{L}_g}{\text{minimize:}} \quad f(g_{\Theta_l}, c_{\mathcal{W}_q}) + \sum_t \lambda_t \sum_l \Phi_t(\Theta_l), \quad (6)$$

where $c_{\mathcal{W}_q}$ represents the forward path of a Conv2D layer (with layer index q); the second term in Eq. (6) denotes the regularization on the complexity of Θ_l , where each constraint Φ_t is weighted by a multiplier $\lambda_t \in (0, 1)$.

In this paper, we propose a subspace model for Θ_l (c.f. Def. 2) and two regularization terms Φ_t ($t = 1, 2$) on the complexity of Θ_l . The subspace model is characterized by its basis vectors (i.e. the eigen-filters) and the corresponding coefficients, which are trained simultaneously using backpropagation.

- **Regularization:** Inspired by Lemma 1, for a given SCEF layer l , we choose two regularizations:

$$\Phi_1 : \quad \lambda_1 \left\| \bar{\mathbf{U}}^{(i)\top} \bar{\mathbf{U}}^{(i)} - \mathbf{I} \right\|_2 \quad (7)$$

$$\Phi_2 : \quad \lambda_2 \left\| \mathbf{a}_j^{(i)} \right\|_2, \quad \mathbf{a}_j^{(i)} = \left[a_{1,j}^{(i)}, \dots, a_{r,j}^{(i)} \right] \quad (8)$$

- **Loss function:** Given a layer Θ_l parameterized by Eq. (3) and the regularizations Φ_t ($t = 1, 2$), we specify

the objective function of the network as follows:

$$\begin{aligned} \underset{\mathbf{a}_j^{(i),l}, \bar{\mathbf{U}}^{(i),l}, l \in \mathcal{L}_g, \mathcal{W}_q, q \in \mathcal{L} \setminus \mathcal{L}_g}{\text{minimize:}} \quad & f\left(g_{\{\mathbf{a}_j^{(i),l}, \bar{\mathbf{U}}^{(i),l}\}}, c_{\mathcal{W}_q}\right) \\ & + \lambda_1 \sum_{i,l} \left\| \bar{\mathbf{U}}^{(i),lT} \bar{\mathbf{U}}^{(i),l} - \mathbf{I} \right\|_2 + \lambda_2 \sum_{i,j,l} \left\| \mathbf{a}_j^{(i),l} \right\|_2 \end{aligned} \quad (9)$$

The choice of the hyperparameters are discussed in the experiments and results section.

Algorithm 1. (*SCEF-basenet*)

Step 1: Choose a CNN topology as *basenet*.

Step 2: Replace any Conv2D layers by *SCEF* layers with hyperparameters r, λ_1, λ_2 .

Step 3: Initialization for each *SCEF* layer ($k = 1, \dots, r$):

- Eigen-filters $\mathbf{u}_k^{(i)}$:
 - Generate random matrices: $\mathbf{A}^{(i)} \in \mathbb{R}^{K \times r}$, $K = h^2$.
 - Compute the truncated SVD: $\mathbf{A}^{(i)} = \bar{\mathbf{U}}^{(i)} \bar{\mathbf{S}}^{(i)} \bar{\mathbf{V}}^{(i)T}$.
 - Reshape each column in $\bar{\mathbf{U}}^{(i)}$ into matrix $\mathbf{u}_k^{(i)} \in \mathbb{R}^K$.
- Coefficients $a_{k,j}^{(i)}$: randomly initialized from a normal distribution.

Step 4: Forward path and training

- Forward path $\mathbf{I}_l \rightarrow \mathbf{I}_{l+1}$: for each output channel j ,

$$\mathbf{I}_{l+1}^j = \sum_{i=1}^{c_{in}} \sum_{k=1}^r a_{k,j}^{(i),l} \mathbf{u}_k^{(i),l} * \mathbf{I}_l^i$$

- Training: backpropagation with the loss function described in Eq. (9).

2.3.2 Use case 2: compressing a trained CNN

In some applications, retraining a CNN is not feasible, but we are still interested in compressing the trained CNN to reduce the runtime complexity. In this case, we propose a compression algorithm as follows.

Algorithm 2. (*SCEFC-basenet*)

Step 1: Analysis described in Procedure 1.

Step 2: For each layer, let $\bar{\mathbf{u}}_k^{(i)}$ be the columns of $\bar{\mathbf{U}}^{(i)}$. Approximate $\mathbf{w}_j^{(i)}$ by $\mathbf{w}_j^{(i)} \approx \sum_{k=1}^{r_i} a_{k,j}^{(i)} \mathbf{u}_k^{(i)}$, where $\mathbf{u}_k^{(i)}$ is obtained by reshaping $\bar{\mathbf{u}}_k^{(i)}$ into a $h \times h$ matrix.

Step 3 (optional): Network fine-tuning by freezing the eigen-filters and training the other trainable parameters.

3. Related Work

It has been found that many deep neural networks suffer from heavy over-parametrization [6], which results in inefficient computational power consumption and memory utilization. This problem has been addressed with several existing approaches.

Pruning: Pruning refers to techniques that aim at reducing the number of parameters in a pre-trained network by identifying and removing redundant weights. In Optimal Brain Damage by LeCun et al. [21], and later in Optimal Brain Surgeon by Hassibi et al. [11], redundant weights are defined by their impact on the objective function, which are identified using the Hessian of the loss function. Other definitions of redundancy have been proposed in subsequent work. For instance, Anwar et al. [1] applies pruning on the filter-level of CNNs by using particle filters to propose pruning candidates. Han et al. [10] introduces a simpler pruning method using a strong L2 regularization term, where weights under a certain threshold are removed. Molchanov et al. [25] uses Taylor expansion to approximate the influence in the loss function by removing each filter. Li et al. [22] identifies and removes filters having a small effect on the accuracy. More recently, in [23] and [24], Luo et al. analyzes the redundancy of filters in a trained network by looking at statistics computed from its next layer. He et al. [14] proposes an iterative LASSO regression based channel selection algorithm. Huang et al. [15] removes filters by training a pruning agent to make decisions for a given reward function. In [32], Yu et al. poses the pruning problem as a binary integer optimization and derives a closed-form solution based on final response importance.

Architectural design: Effort has been put into designing a smaller network architecture without loss of the generalization ability. For instance, He et al. [12] achieves a higher accuracy compared to other more complex networks by introducing the residual building block. The residual building blocks adds an identity mapping that allows the signals to be directly propagated between the layers. Iandola et al. [16] introduces SqueezeNet and the Fire module, which is designed to reduce the number of parameters in a network by introducing 1×1 filters. Recently, Xie et al. [31] proposed a multi-branch architecture which exposes a new hyperparameter for each block to effectively control the capacity of the network.

Compression: Deep Compression, by Han et al. [9], reduces the storage size of the model using quantization and Huffman encoding to compress the weights in the network. Other work on reducing the memory size of models is done by binarization. In XNOR-Net by Rastegari et al. [27], the

weights are reduced to a binary representation and convolutions are replaced by XNOR operations. More recently, Suau et al. [28] proposed to analyze filter responses to automatically select compression methods for each layer.

Subspace techniques: Subspace properties of trainable filters in CNNs are explored. Sometimes, this is referred to Low-Rank Approximation (LRA) in the literature. There are mainly two different implementations in the LRA approach. 1) *Separable bases*: Jaderberg et al. [18] decomposes the $d \times d$ filters into $1 \times d$ and $d \times 1$ filters to construct rank-1 bases in the spatial domain. Later, Tai et al. [29], finds a closed form solution to this factorization. Ioannou et al. [17] introduces a novel weight initialization that allows small basis filters to be trained from scratch, which has achieved similar or higher accuracy than the traditional conventional CNNs. Yu et al. [33] proposes a SVD-free algorithm that uses the idea that filters usually share smooth components in a low-rank subspace. 2) *Filter vectorization*: Some existing work implements the low rank approximation by vectorizing the filters. For instance, Denton et al. [7] stacks all filters for each output channel into a high dimensional vector space and approximates the trained filters using SVD. Wen et al. [30] presents a regularization to enforce filters to coordinate into lower-rank space, where the subspaces are constructed from all the input channels for each given output channel. Recently, Peng et al. [26] proposed a decomposition focusing on exploiting the filter group structure for each layer.

Weight sharing: Another approach to reduce the number of parameters in a network is to share weights between the filters and layers. Boulch [3] share weights between the layers in a residual network operating on the same scale.

Depthwise separable convolutions: introduced by Chollet [4], have shown to be a more efficient use of parameters compared to regular Conv2Ds Inception like architectures. Depthwise separable convolutions have also been used in other work, e.g., in [14] by He et al., where it was used to gain a computational speed-up of ResNet networks.

Our focus: To have an empirically comparison to the state-of-the-art techniques, we choose a popular base network (i.e. ResNet) and compare our experimental results to various modifications of the base network implemented by the aforementioned techniques.

4. Experiments and Results

4.1. Deterministic rule-based hyperparameters

We choose the hyperparameters based on deterministic rules to avoid hyperparameter tuning and to increase reproducibility. These rules are determined using a transfer learning approach. First, we find the hyperparameters in SCEF using cross-validation on a small dataset CIFAR-10, where cross-validation is affordable. Then we establish a rule for each hyperparameter. These rules are then directly

applied to the larger dataset ImageNet without tuning.

There are three sets of hyperparameters $h1 \sim h3$:

h1: Ranks r (Algo. 1): The observation of singular values (c.f. Fig. 1) from several networks and datasets shows that the effective ranks are typically decreasing with respect to the “depth” of the layers, i.e., layers at the beginning of the network often have higher rank, and vice versa. In this paper, we adopt two alternative routines for choosing the rank in each layer: linear decay and logarithmic decay shown in Fig. 4. Let l be the depth index of a layer and $K = h^2$.

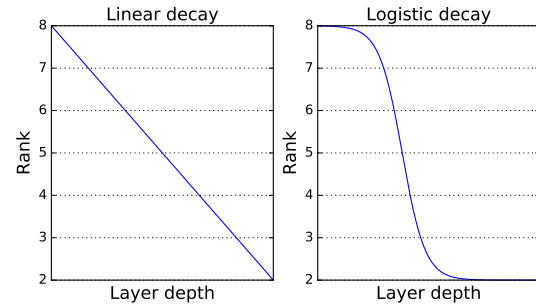


Figure 4: Choosing rank using linear decay and logarithmic decay.

Denote $l_{\max} = \max(l)$ and $l_{\min} = \min(l)$.

- Linear decay: $\hat{r}_i = \left\lfloor \frac{l(K-1)}{l_{\max}-l_{\min}} \right\rfloor$.
- logarithmic decay: $\hat{r}_i = \left\lfloor \frac{K-1}{\log_2(l)} \right\rfloor$.

h2: Regularization coefficients (Algo.1, cf. Eq. (7), (8)): $\lambda_1 = 0.001r$ and $\lambda_2 = 0.001$.

h3: Singular value threshold (Algo.2, cf. Eq. (2)): $\gamma = 0.3$.

4.2. Hardware

For training and experiments, Nvidia DGX-1s with Intel Xeon E5-2698 v4 2.2 GHz CPUs and Nvidia Tesla V100 SXM2 with 32 GB of GPU memory are used.

4.3. Dataset CIFAR-10: Ablation Study

Dataset: To empirically study the behavior of SCEF, we conduct various experiments on the standard image recognition dataset CIFAR-10 by Krizhevsky and Hinton [20].

Benchmark: We use ResNet-32 as the base network for comparison. ResNet-32 has three **blocks** as shown in Fig. 2, where the last block (block-3) in ResNet-32 has the most filters. Since our goal is to reduce the amount of trainable parameters and FLOPs, we mainly vary the structure in block-3 in our experiments.

Results: The results are presented in terms of the estimated mean and the standard deviation of the classification accuracy on the testing set with 10 runs for each experiment setup,

which are shown in Fig. 5 and Fig. 6. The accuracy is then presented with respect to the number of trainable parameters for each network structure. For SCEF layers, there are nine data points in each presented result, which correspond to different layer ranks in block-3 $r_3 \in \{1, \dots, 9\}$. In addition, the number of trainable parameters in SCEF layers is also varied by using different numbers of output channels in block-3, i.e., $c_{\text{out}} \in \{64, 96, 128\}$. We then vary c_{out} in ResNet-32 block-3 ($c_{\text{out}} \in \{16, 20, 24, \dots, 128\}$) to have a comparable result. We compare the accuracy achieved by SCEF-ResNet-32 Fig. 7. More results can be found in the supplementary material.

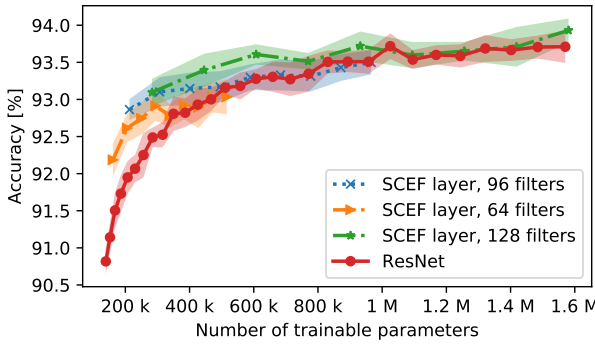


Figure 5: Accuracy versus number of parameters for different network structures for the CIFAR-10-dataset.

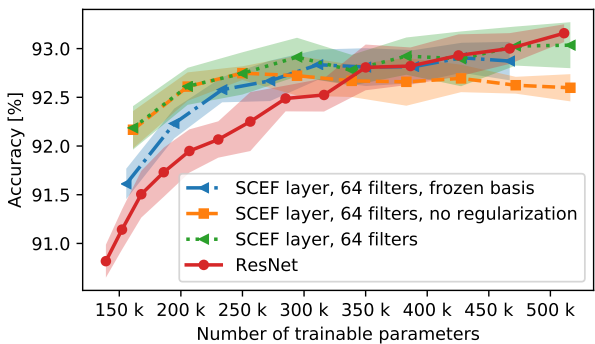


Figure 6: (1) trainable eigen-filters with regularization, (2) frozen eigen-filters with regularization, (3) trainable eigen-filters without regularization the for CIFAR-10-dataset.

Experiment 1. Varying rank r and c_{out} : For a layer with input channels $i = 1, \dots, c_{\text{in}}$ and output channels $j = 1, \dots, c_{\text{out}}$, the filters in the SCEF layer is expressed as $\mathbf{w}_j^{(i)} = \sum_{k=1}^r a_{k,j}^{(i)} \mathbf{u}_k^{(i)}$. We empirically show that SCEF layers achieve higher accuracy with significantly lower number of parameters. In this experiment, we vary two hyperparameters: 1) the rank r of each filter in the SCEF layer, and 2)

the number of output channels c_{out} . We compare the accuracy versus the number of parameters in different types of layers (Conv2D and SCEF with different hyperparameters). As shown in Fig. 5, with a lower number of parameters, SCEF achieves a better accuracy with low rank approximation. Moreover, when we increase the number of output channels, SCEF shows a even more promising result with fewer parameters in total.

Experiment 2. Trainable vs frozen eigen-filters: In Algo. 1, the eigen-filters in SCEF layers are trained simultaneously using backpropagation. In this experiment, we investigate the impact of this training process and try to understand **if it is sufficient to use random basis vectors as eigen-filters**. We initialize the eigen-filters according to Algo. 1 and freeze them during training. The comparison between the accuracies achieved by frozen (dotted) and trainable (dashed) eigen-filters can be found in Fig. 6. By using frozen eigen-filters, the network has a fewer number of trainable parameters for the same rank. With a low rank ($r < 5$), the accuracy is degraded without training.

Experiment 3. With or without Φ_1 regularization: To study the effect of the Φ_1 regularization introduced in Eq. (7), some experiments can be found in Fig. 6. We can see that with a high rank, the regularization needs to be applied. In our experiment, we use $\lambda_1 = 0.0001r$ and $\lambda_2 = 0.0001$, where λ_1 is the multiplier of the constraint on the eigen-filters and λ_2 is on the subspace coefficients. The reason for having the multiplier r in λ_1 is to suppress the growth of the cost when r becomes large.

Experiment 4. Comparison to related work: In this experiment, we implement Algo. 1 (SCEF-ResNet-32) to compared to the state-of-the-art techniques. We vary the number of output channels c_{out} in the last ResNet block for comparison, where we see that having fewer eigen-filters with more output channels yields a better result.

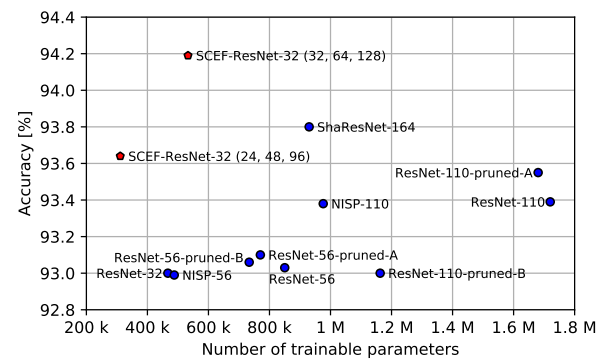


Figure 7: Comparison of accuracy versus the number of trainable parameters of related work for CIFAR-10. In the parenthesis, we show the number of output channels in each ResNet block.

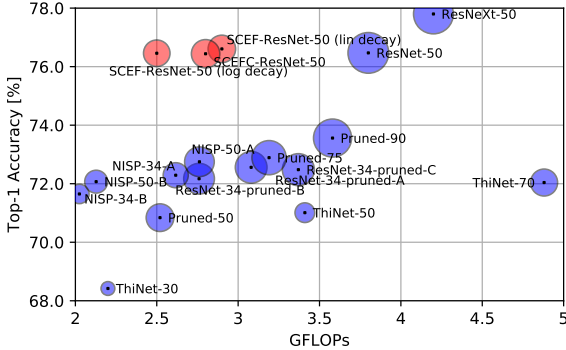


Figure 8: Top-1 accuracy (y-axis) versus FLOPs (x-axis) and number of trainable parameters (indicated by the radius of each disk) for ImageNet. In this figure, we show how SCEF-ResNet-50 compares to other ResNet-50 variant networks ([31, 22, 31, 32, 24, 23, 13]). See supplementary material for detailed results.

4.4. Dataset ImageNet (ILSVRC-2012)

To further compare our algorithms to the state-of-the-art, we use the standard dataset ImageNet (ILSVRC-2012) by Deng et al. [5]. ImageNet is a dataset with 1.2 M training images and 50 k validation images of 1000 object classes, commonly evaluated by top-1 and top-5 accuracy. We use ResNet-50 v2 [13] as the base network for both use case 1&2. The results are visualized in Fig. 8 for top-1 accuracy and Fig. 9 for top-5 accuracy, respectively. The ranks used in SCEF-ResNet-50 (use case 1) and SCEFC-ResNet-50 (use case 2) are determined by the deterministic rules presented in **h1**, **h2** and **h3**. In particular, the ranks for SCEFC-ResNet-50 are: block 1: (4, 4, 7), block 2: (1, 4, 7, 6), block 3: (1, 4, 6, 6, 4) and block 4: (1, 1, 1). For each setup, we have five runs and report the average accuracy and its standard deviation. From the experiments, we see the trade-off between the two rank decay mechanisms: linear decay is less aggressive, which yield to a better accuracy, whereas logarithmic decay reduce a greater number of FLOPs while still having a decent accuracy.

5. Conclusion and future work

Motivated by our observations of the low rank behaviors in a CNN, in this paper, we present a layer structure SCEF as an alternative parameterization to Conv2D using the depthwise separable convolution and subspace approximation techniques. SCEF can be used to build a network from scratch by training the eigen-filters and the coefficients or to compress trained networks. Our experiments show that it is important to allow training of the eigen-filters to achieve the highest accuracy. In addition, we observe that

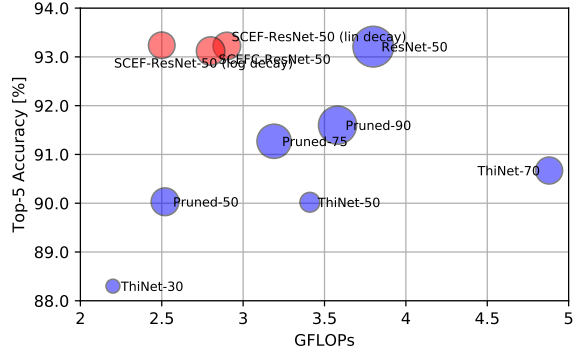


Figure 9: Top-5 accuracy (y-axis) versus FLOPs (x-axis) and number of trainable parameters (indicated by the radius of each disk) for ImageNet. In this figure, we show how SCEF-ResNet-50 compares to other ResNet-50 variant networks ([33, 3, 31, 32, 24, 23, 13]). See supplementary material for detailed results.

in terms of the accuracy-to-complexity ratio, it is beneficial to use more coefficients (i.e. output channels) with fewer eigen-filters (i.e. lower rank) in SCEF layers. The SCEF layer is simple to implement using depthwise separable convolutions that are recently made available in common deep learning frameworks and gaining popularity due to its computational efficiency. Moreover, with the deterministic rules for choosing hyperparameters, it is easy to design and reproduce the results. From our observation, the underlying subspace structure is a commonly shared property amongst different network topologies, which provides insights to the design of CNNs and analyses of their redundancies. As a future direction, we will further explore and analyze this underlying structure and improve our design strategies using transfer learning techniques.

References

- [1] S. Anwar, K. Hwang, and W. Sung. Structured pruning of deep convolutional neural networks. *J. Emerg. Technol. Comput. Syst.*, 13(3):32:1–32:18, Feb. 2017. ISSN 1550-4832. doi: 10.1145/3005348. 6
- [2] P. Belhumeur, J. Hespanha, and D. Kriegman. Eigenfaces vs fisher faces recognition using class specific linear projection. *IEEE Transactions on Pattern Analysis and Machine Intelligence*, 19:711–720, 1997. 1
- [3] A. Boulch. Reducing parameter number in residual networks by sharing weights. *Pattern Recognition Letters*, 103:53 – 59, 2018. ISSN 0167-8655. doi: <https://doi.org/10.1016/j.patrec.2018.01.006>. 7, 9
- [4] F. Chollet. Xception: Deep learning with depthwise separable convolutions. In *The IEEE Conference on Computer Vision and Pattern Recognition (CVPR)*, July 2017. 2, 3, 7

[5] J. Deng, W. Dong, R. Socher, L. Li, K. Li, and L. Fei-Fei. Imagenet: A large-scale hierarchical image database. In *2009 IEEE Conference on Computer Vision and Pattern Recognition*, pages 248–255, June 2009. doi: 10.1109/CVPR.2009.5206848. 9

[6] M. Denil, B. Shakibi, L. Dinh, M. Ranzato, and N. de Freitas. Predicting parameters in deep learning. In *Proceedings of the 26th International Conference on Neural Information Processing Systems - Volume 2*, NIPS’13, pages 2148–2156, USA, 2013. Curran Associates Inc. URL <http://dl.acm.org/citation.cfm?id=2999792.2999852>. 6

[7] E. L. Denton, W. Zaremba, J. Bruna, Y. LeCun, and R. Fergus. Exploiting linear structure within convolutional networks for efficient evaluation. In Z. Ghahramani, M. Welling, C. Cortes, N. D. Lawrence, and K. Q. Weinberger, editors, *Advances in Neural Information Processing Systems 27*, pages 1269–1277. Curran Associates, Inc., 2014. 2, 7

[8] G. Golub and C. van Loan. *Matrix Computations, 3rd edition*. Johns Hopkins Press, 1996. 1

[9] S. Han, H. Mao, and W. J. Dally. Deep compression: Compressing deep neural networks with pruning, trained quantization and huffman coding. *arXiv preprint arXiv:1510.00149*, 2015. 6

[10] S. Han, J. Pool, J. Tran, and W. J. Dally. Learning both weights and connections for efficient neural networks. In *Proceedings of the 28th International Conference on Neural Information Processing Systems - Volume 1*, NIPS’15, pages 1135–1143, Cambridge, MA, USA, 2015. MIT Press. URL <http://dl.acm.org/citation.cfm?id=2969239.2969366>. 6

[11] B. Hassibi, D. G. Stork, and G. J. Wolff. Optimal brain surgeon and general network pruning. In *IEEE International Conference on Neural Networks*, pages 293–299 vol.1, 1993. doi: 10.1109/ICNN.1993.298572. 6

[12] K. He, X. Zhang, S. Ren, and J. Sun. Deep residual learning for image recognition. In *2016 IEEE Conference on Computer Vision and Pattern Recognition (CVPR)*, pages 770–778, June 2016. doi: 10.1109/CVPR.2016.90. 6

[13] K. He, X. Zhang, S. Ren, and J. Sun. Identity mappings in deep residual networks. In *European conference on computer vision*, pages 630–645. Springer, 2016. 9

[14] Y. He, X. Zhang, and J. Sun. Channel Pruning for Accelerating Very Deep Neural Networks. *Proceedings of the IEEE International Conference on Computer Vision*, 2017-Octob: 1398–1406, 2017. ISSN 15505499. doi: 10.1109/ICCV.2017.155. 6, 7

[15] Q. Huang, K. Zhou, S. You, and U. Neumann. Learning to prune filters in convolutional neural networks. *arXiv preprint arXiv:1801.07365*, 2018. 6

[16] F. N. Iandola, S. Han, M. W. Moskewicz, K. Ashraf, W. J. Dally, and K. Keutzer. SqueezeNet: Alexnet-level accuracy with 50x fewer parameters and; 0.5 mb model size. *arXiv preprint arXiv:1602.07360*, 2016. 6

[17] Y. Ioannou, D. Robertson, J. Shotton, R. Cipolla, and A. Criminisi. Training cnns with low-rank filters for efficient image classification. *arXiv preprint arXiv:1511.06744*, 2015. 2, 7

[18] M. Jaderberg, A. Vedaldi, and A. Zisserman. Speeding up convolutional neural networks with low rank expansions. In *Proceedings of the British Machine Vision Conference*. BMVA Press, 2014. doi: <http://dx.doi.org/10.5244/C.28.88>. 2, 7

[19] I. T. Jolliffe. Principal component analysis. *Springer-Verlag*, 1986. 1

[20] A. Krizhevsky and G. Hinton. Learning multiple layers of features from tiny images. Technical report, Citeseer, 2009. 7

[21] Y. LeCun, J. S. Denker, and S. A. Solla. Optimal brain damage. In D. S. Touretzky, editor, *Advances in Neural Information Processing Systems 2*, pages 598–605. Morgan-Kaufmann, 1990. URL <http://papers.nips.cc/paper/250-optimal-brain-damage.pdf>. 6

[22] H. Li, A. Kadav, I. Durdanovic, H. Samet, and H. P. Graf. Pruning filters for efficient convnets. *arXiv preprint arXiv:1608.08710*, 2016. 6, 9

[23] J.-H. Luo and J. Wu. An entropy-based pruning method for cnn compression. *arXiv preprint arXiv:1706.05791*, 2017. 6, 9

[24] J.-H. Luo, J. Wu, and W. Lin. Thinet: A filter level pruning method for deep neural network compression. In *Proceedings of the IEEE international conference on computer vision*, pages 5058–5066, 2017. 6, 9

[25] P. Molchanov, S. Tyree, T. Karras, T. Aila, and J. Kautz. Pruning convolutional neural networks for resource efficient transfer learning. *arXiv preprint arXiv:1611.06440*, 2016. 6

[26] B. Peng, W. Tan, Z. Li, S. Zhang, D. Xie, and S. Pu. Extreme network compression via filter group approximation. In *Proceedings of the European Conference on Computer Vision (ECCV)*, pages 300–316, 2018. 2, 7

[27] M. Rastegari, V. Ordonez, J. Redmon, and A. Farhadi. Xnornet: Imagenet classification using binary convolutional neural networks. In B. Leibe, J. Matas, N. Sebe, and M. Welling, editors, *Computer Vision – ECCV 2016*, pages 525–542, Cham, 2016. Springer International Publishing. ISBN 978-3-319-46493-0. 6

[28] X. Suau, L. Zappella, and N. Apostoloff. Network Compression using Correlation Analysis of Layer Responses. 2018. URL <http://arxiv.org/abs/1807.10585>. 7

[29] C. Tai, T. Xiao, Y. Zhang, X. Wang, et al. Convolutional neural networks with low-rank regularization. *arXiv preprint arXiv:1511.06067*, 2015. 2, 7

[30] W. Wen, C. Xu, C. Wu, Y. Wang, Y. Chen, and H. Li. Coordinating filters for faster deep neural networks. In *The IEEE International Conference on Computer Vision (ICCV)*, Oct 2017. 2, 7

[31] S. Xie, R. Girshick, P. Dollár, Z. Tu, and K. He. Aggregated residual transformations for deep neural networks. *Proceedings - 30th IEEE Conference on Computer Vision and Pattern Recognition, CVPR 2017*, 2017-January:5987–5995, 2017. doi: 10.1109/CVPR.2017.634. 6, 9

[32] R. Yu, A. Li, C.-F. Chen, J.-H. Lai, V. I. Morariu, X. Han, M. Gao, C.-Y. Lin, and L. S. Davis. Nisp: Pruning networks using neuron importance score propagation. In *The IEEE Conference on Computer Vision and Pattern Recognition (CVPR)*, June 2018. 6, 9

[33] X. Yu, T. Liu, X. Wang, and D. Tao. On compressing deep models by low rank and sparse decomposition. In *The IEEE Conference on Computer Vision and Pattern Recognition (CVPR)*, July 2017. 2, 7, 9